ARMY RESEARCH LABORATORY

Evaluation of Spectra Airlift Sling Systems Subjected to Asymmetric Fatigue Loading

Robert B. Dooley, Robert E. Pasternak,
Charles Pergantis, and Dr. J.L. Mead

ARL-TR-757

June 1995

REPORT DOCUMENTATION PAGE

Form Approved
OMB No. 0704-0188

1. AGENCY USE ONLY (Leave blank)	2. REPORT DATE	3. REPORT TYPE AND DATES COVERED
	June 1995	11/93 - 6/95

4. TITLE AND SUBTITLE Evaluation of Spectra Airlift Sling Systems Subjected to Asymmetric Fatigue Loading

5. FUNDING NUMBERS

6. AUTHOR(S)

Robert B. Dooley, Robert E. Pasternak, Charles Pergantis, and Dr. J.L. Mead

7. PERFORMING ORGANIZATION NAME(S) AND ADDRESS(ES)

Army Research Laboratory
Watertown, MA 02172-0001
ATTN: AMSRL-MA-PA

8. PERFORMING ORGANIZATION REPORT NUMBER

ARL-TR-757

9. SPONSORING/MONITORING AGENCY NAME(S) AND ADDRESS(ES)

10. SPONSORING/MONITORING AGENCY REPORT NUMBER

11. SUPPLEMENTARY NOTES

12a. DISTRIBUTION/AVAILABILITY STATEMENT

Approved for public release; distribution unlimited.

12b. DISTRIBUTION CODE

13. ABSTRACT *(Maximum 200 words)*

The contents of this report describe the results and observations of experimental activities focused on evaluating the performance of SPECTRA™ Airlift Sling Systems in support of an External Airlift Transportation (EAT) failure investigation. One of two legs of the twin leg SPECTRA sling system was subjected to fatigue loading in an asymmetric test configuration (four sling systems fatigued). Ultimate strength tests were performed on the fatigued legs to determine reduced strength. An additional two slings were reserved to identify virgin (non-fatigued) ultimate strength. Test parameters including cable gender loading (ie. male versus female sling leg), splice coatings, and the effects of heat and degradation of strength by fatigue were examined. Attempts were made to identify the most influential test parameters. Correlations between ultimate strength and the test parameters were established.

14. SUBJECT TERMS	15. NUMBER OF PAGES
Airlift, Sling, Cable	27
	16. PRICE CODE

17. SECURITY CLASSIFICATION OF REPORT	18. SECURITY CLASSIFICATION OF THIS PAGE	19. SECURITY CLASSIFICATION OF ABSTRACT	20. LIMITATION OF ABSTRACT
Unclassified	Unclassified	Unclassified	UL

NSN 7540-01-280-5500

Standard Form 298 (Rev. 2-89)
Prescribed by ANSI Std. Z39-18
298-102

CONTENTS

Page

INTRODUCTION 1

DESCRIPTION OF SPECTRA AIRLIFT SLING SYSTEM 1

ANALYSIS OF THE FAILED AIRLIFT SLING LOOP 2

TEST PARAMETER IDENTIFICATION 2

ASSYMETRIC FATIGUE TEST SET-UP 3

ULTIMATE STRENGTH TESTING 5

TEST RESULTS

Mechanical 6

Calculations 6

Temperature, Heat and Energy 8

Observations 10

CONCLUSIONS 11

ACKNOWLEDGEMENTS 12

TABLE OF FIGURES 13

APPENDIX I,

Thermodynamic Properties and Chemical Identification . . 14

INTRODUCTION

This investigation was undertaken as a consequence of an External Airlift Transportation (EAT) operation failure involving an CH-47D helicopter, two twin leg SPECTRA^{TM} Airlift Sling systems (mfg. by Ocean Products Inc.) and a classified prototype EAT cargo load. Evidence collected both during the failure and after recovery operations indicated that the forward sling system failed while flying at moderate speeds and while negotiating a gentle constant altitude turn.

The task of labeling and identifying the position of recovered sling components was performed by members of the flight crew immediately after the failure. Details of flight speeds, cargo weight and maneuvers performed prior to failure were collected and autographically recorded. A video tape recording from a Forward Looking Infrared (FLIR) camera directed at the cargo was used to compliment the evidence and to assist in designing a reconstruction of events under laboratory conditions.

Reports indicate ultimate strength tests of identical sling systems were performed (prior to this incident) in a two point symmetric airlift configuration. Results of these tests indicated a load carrying capacity of approximately 79,200 lbs. per sling system. Static cargo weight was reported to be slightly over 11,600 lbs. Recovered metallic sling shackles with a rated working load capacity of 8,000 lbs. (4 used per operation) were fully functional after the accident indicating that aerodynamically induced cable loads were not excessive.

DESCRIPTION OF THE SPECTRA AIRLIFT SLING SYSTEM

This particular EAT operation involved two twin leg SPECTRA Airlift Sling Systems, one forward and one aft, both of which support the cargo by means of shackles pinned to the ends of the sling legs. Individual slings are supported in the center "loop section" by the helicopter airlift hooks (Figure 1).

The main cable consists of twelve tows of SPECTRA^{TM}(highly oriented, ultra-high molecular weight polyethylene fibers) braided or woven together to produce an overall diameter of approximately 1-1/8". A Samson Brummull splice (Figure 2) is employed at the center of the cable to produce a "loop" of cable protected by a flexible fiberglass sheath. The entire splice section, including the loop, is then coated with a polymeric potting compound to protect the splice and to aid in maintaining the shape of the loop.

At the ends of each leg, the cable makes one wrap around a 2.00" diameter pulley. The SPECTRA^{TM}tows are then individually spliced back into the main cable over a length of approximately

three feet. These end splice sections are covered with a thin protective braided wrapping from the pulley area to slightly beyond the end of the splice.

ANALYSIS OF THE FAILED AIRLIFT SLING LOOP

The splice/loop section of the recovered forward sling appeared externally intact with the internal SPECTRA™ cable having been pulled through and removed. In contrast to the forward loop section, the rear loop appeared deformed with a crumpled sheath section causing an overall reduction in size. The rear splice loop retained the internal SPECTRA™ cable. Rear cables retained their position in the loop due to a load release that occurred when both rear cable legs were severed during the accident from contact with sharp edges of the cargo load.

Radiographs of the forward sling loop area indicated a region of differing density in the potting compound. This observation implied that the area may have contributed to the failure by means of changed material properties. A section of the potting compound was removed by means of a water jet for the purpose of sampling internal material (Figure 3). Visual observations of this section showed what appeared to be a film of melted translucent material with torn SPECTRA™ fibers cast into the potting compound. Chemical analysis of the specimen resulted in the identification of this film as Vinyl Chloride,(later identified as a component of a tape overwrap: ref. Appendix I).

Detailed examinations of various SPECTRA™ cable specimens were performed by using a Wild Macroskop M420 light microscope. Photomicrographs were taken of cable samples collected from various locations along a recovered sling leg. Comparisons of the specimens displayed the effect of abrasion within the splice area on individual fibers. In most cases, specimens collected near the splice show fiber breakage and or fiber splitting. Hard nodular ends on some fibers were observed indicating that high temperatures (possible melting) had been achieved.

TEST PARAMETER IDENTIFICATION

Evaluation of recovered sling components in addition to an analysis of the sling design resulted in the identification of two application characteristics consequently designated as test parameters.

The most influential parameter was believed to be that of the effect of high frequency asymmetric fatigue loading on the integrity of the cable system material. This parameter was believed to contribute to the reduction of sling strength due to internal fiber abrasion from the splice - potting compound interface. It was also believed that this effect may have been compounded by a weakening of the remaining material due to the associated heat generated by friction.

The second parameter believed to contribute to the failure was the sling systems high sensitivity to cable gender loading. Cable gender was determined by splice construction, one leg being designated as male, the other female depending on each cable leg's departure configuration from the splice area (refer to Figure 2). An inherent characteristic feature of the splice design is the squeezing or locking effect of the splice when loaded. Female cable legs tend to constrict about the male leg when loaded. This constriction effect was believed to redistribute the force unevenly among the cables in the splice area (thereby possibly overloading one of the two cables). Overloading of this type could result in premature failure if the load bearing cable sections (tows) in the splice area have been worn from the abrasion described above.

Virgin (non-fatigued) males and females were to be tested against fatigued males and females. Significant strength differences were anticipated between those cables having been fatigued and those that were virgin.

ASYMMETRIC FATIGUE TEST SET-UP

Details of the EAT cargo load sling geometry and the dimensions of the unloaded sling legs were provided by Natick Research Development & Engineering Center. Calculations indicated that in straight level 1.0G flights, the angle between the male and female legs of a single sling system was approximately 30 degrees. Duplication of this angle was achieved in a four post MTS test machine through the use of an outrigger beam secured to the test platen (Figure 4).

Testing loads, for both the static leg and the fatigued leg, were selected by calculating the equivalent static cargo forces for a 1.0G load (3,000 lb.) and for a 3.2G load (9,600 lb.). The 3.2G load factor was chosen as the minimum acceptable upper limit as required in airlift applications by MIL-STD-209G.

Monitoring static and fluctuating loads during testing was accomplished by means of two loads cells. The main load cell (MTS load cell) was positioned within the test machine crosshead and supported the center loop section of the sling. This load cell monitored the force applied to the fatigued leg in addition to the vertical component of the static leg. A second load cell was positioned at the end of the outrigger beam and supported only the static 1.0G load.

Force resolution calculations for this sling geometry indicated that the outrigger leg, (loaded to 1.0G or 3,000 pounds) contributed a static load of 2,600 lbs to the main load cell when stationary. This load was considered as an offset value when programming the control equipment. Consequently, values for the fatigue leg at 1.0 and 3.2G loads were 5,600 and 12,200 lb. respectively. Load application for the fatigue leg was driven by a signal emitted by a digital function generator.

Heat generation near the splice area was monitored during testing by means of an Inframetrics™ thermographic infrared (IR) thermal imaging camera. Finite local splice temperatures were monitored by type "J" thermocouples cast into the potting compound such that the sensing tip was located approximately 1.0 inch away from the splice. On unpotted slings, the thermocouples were mounted on the surface of the cable about 1/2 inch away from the splice. Actual locations of thermocouple tips varied from specimen to specimen and were confirmed to be within a reasonable distance from the splice via pretest radiographs.

The IR camera was directed at the splice area with a field of view large enough to include the loop area with an additional two feet of each cable leg. Ambient laboratory temperatures were monitored by an additional thermocouple mounted approximately two feet away from the sling.

An additional technique of quantifying the amount of heat energy generated by the entire system was employed by means of collecting and integrating load versus displacement data for a series of cycles after the 39 hour mark. The necessary instrumentation was prepared in an effort to generate hysteresis loops to determine if energy was continually being stored in the cable legs or if thermal (via strain) equilibrium had been achieved. Conservation of energy equations were then employed to determine the global temperature increase of the system. To perform this calculation, specific heat values of the potting compound and of the SPECTRA™ material were required and were determined via Differential Scanning Calorimitry (DSC) tests. Results are indicated below (Ref., Appendix I).

MATERIAL	SPECIFIC HEAT
Potting compound	1.80 joules/gm^{o}C
Spectra	1.65 joules/gm^{o}C

A practice test was performed on sling #5 (unpotted, i.e. comparably expendable) to determine the maximum possible loading frequency and range at which the tests could be performed. Details of the practice test are outlined below.

SLING #5 [UNPOTTED-FEMALE FATIGUED]
** PRACTICE TEST **

static	lb.	3,300$_{+}$	(male)
cyc. range	lb.	3,000-9,600	(female)
MTS cell	lb.	5,600-11,600*	(system)
frequency	cps.	10.0	(female)
leg angle	deg.	30	(system)
total cycles	#	188,737	(female)
observed temp.	^{o}F	76-86	(splice)

(+ 300 lbs. extra to compensate for anticipated decay)
(* 600 lbs. less than 3.2G, minimized static decay)

Excessive elongation of the fatigued leg, in addition to the load decay of the static leg, limited the practical operating frequency to a maximum of 10.0 cycles per second.

As there was minimal apparent damage to the splice and fibers of sling #5, a modification to the test plan was required. A test loading spectrum outlined in a report from the Aviation Applied Technology Directorate detailing the fatigue testing of Kaman/Cortland SPECTRA slings (prototype) was selected. This test load spectrum was modified slightly for adaptation to ARL-MD test equipment. A description of the test schedule is outlined below.

Modified Test Load Schedule

1. Statically apply load to 1.0G in each leg (via crosshead displacement and actuator)
2. Apply and maintain sinusoidal load (fatigue leg only) at 5 cycles/sec with 1,000 lb peak to peak, (1G mean load). (actuator only)
3. Move mean load to 4.8G (@ max stroke speed) and maintain for 20 seconds. (fatigue leg-actuator only)
4. Move mean load to 1.0G (@ max stroke speed) and maintain for 1 hour.(fatigue leg-actuator only)
5. Move mean load to 3.2G (@ max stroke speed) and maintain for 3 min., 20 sec.(fatigue leg-actuator only)
6. Move mean load to 1.0G (@ max stroke speed) and maintain for 1 hour.(fatigue leg-actuator only)
7. Move mean load to zero load over approximately 10 seconds (slack the fatigue leg-actuator only)
8. Return to step #3, and repeat for 40 hours.

where;

Step #3	simulates rapid lift-off
Step #4,#6	simulates level flight
Step #5	simulates 3.2G turn
Step #7	simulates landing

Figure 5a,b shows the practice test load versus time plots for the main and static load cells with sling #5 subjected to the modified plan. Each of the four fatigue slings were tested in accordance with this loading schedule for approximately 40 hours, including sling #5 (totaling approximately 80 hours from two tests).

ULTIMATE STRENGTH TESTING

Ultimate strength testing of the four fatigued slings and the two virgin slings was performed in a BALDWIN 600,000 lb capacity hydraulic test machine. A four inch diameter steel pin was positioned in the upper crosshead of the machine to simulate the actual dimensions of an CH-47D helicopter cargo hook. The upper pin supported the loop section of each test sling. The bottom end of each test leg, corresponding to the leg that was subjected to fatigue loads, was constrained in the lower

crosshead by means of a through bolt supporting the two inch diameter pulley. In each test, the static leg was allowed to hang freely beside the fatigued test leg. Virgin legs, both male and female, were tested in a similar fashion.

As excessive elongation was anticipated, a preload of approximately 21,000 lbs. was applied to each test leg by means of electro-mechanically displacing the lower crosshead. This precaution allowed test engineers to utilize the maximum upper crosshead stroke for loading to failure via hydraulic crosshead displacement.

A Linear Voltage Displacement Transducer (LVDT) was positioned beneath the lower crosshead to measure crosshead displacement (elongation) of each tested sling leg.

TEST RESULTS

Mechanical

Ultimate strength and elongation data collected from the tests are shown in Table 1.

CALCULATIONS

Calculations performed on data from Table 1 indicate the following:

AVERAGE FATIGUED MALE STRENGTH......................23,140 lbs.
AVERAGE FATIGUED FEMALE STRENGTH....................33,575 lbs.
*[female to male strength ratio: 1.45]

AVERAGE FATIGUED MALE ELONGATION......................4.05 in.
AVERAGE FATIGUED FEMALE ELONGATION...................15.30 in.
*[female to male elongation ratio: 3.78 (fatigued)]

VIRGIN MALE ELONGATION................................9.00 in.
VIRGIN FEMALE ELONGATION.............................17.40 in.
*[female to male (virgin) elongation ratio: 1.93 (virgin)]

AVERAGE FATIGUED MALE SPRING STIFFNESS (K_m).......5,714 lbs./in.
AVERAGE FATIGUED FEMALE SPRING STIFFNESS (K_f).....2,194 lbs./in.
*[female to male stiffness ratio: 0.384]
(average spring stiffness, 2,147 lbs./in.)

VIRGIN MALE SPRING STIFFNESS ($K_{m,v}$)...............2,564 lbs./in.
VIRGIN FEMALE SPRING STIFFNESS ($K_{f,v}$).............1,729 lbs./in.

AVERAGE FATIGUED SPRING CONSTANT RATIO
MALE TO FEMALE 2.6
FEMALE TO MALE 0.385

ULTIMATE STRENGTH TEST RESULTS

sling #	potting	gender	history	elongation of test leg (in.)	load at failure (lb.)
1	yes	female	fatigued	15.30	33,400
2	yes	male	fatigued	4.50	22,480
3	yes	female	virgin	17.4	30,100
4	yes	male	virgin	9.00	23,080
5	no	female	fatigued	15.30	33,750
6	no	male	fatigued	3.60	23,800

Based on the data above, the following observations can be made and apply to springs supporting loads in a parallel configuration (modeling this application).

$$K_{effective} = K_m + K_f = 7,908 \text{ lbs./in.}$$

For equally distributed cargo loads (ie. static 1.0G load) the forward sling system supports approximately 6,000 lbs. According to even deflection conditions, neglecting the effect of the 30 degree angle, and supporting this load, the following was determined:

SLING LEGS (BOTH): 0.759 inch deflection @ 6000 lb.

Load distributions between the male and female legs subjected to a constant even deflection of 0.759 inches indicate the following:

male supports	....	4,335 lbs.
female supports	....	1,665 lbs.
	TOTAL	6,000 lbs.

Results of these calculations indicate that if the cargo is maintained at a level orientation with respect to the horizon, the male leg carries 160% more of the load as compared to the female. During 3.2G maneuvers, and under even deflection conditions, the male leg supports 13,872 pounds. The factor of safety for this load based on ultimate strength tests results is 1.6 (using fatigued male leg data).

Temperature, Heat and Energy

During manufacturing of the potted slings, thermocouples cast into the black potting compound were monitored via a remote type "J" thermocouple signal converter. Maximum temperatures recorded during the pouring and curing operations are listed below.

SLING	MAX. Recorded Temp
sling #1	84 °F
sling #2	86 °F
sling #3	69* °F
sling #4	68* °F

*= insufficient data available

Attempts to determine the global temperature increase of the sling systems (during fatigue testing) failed as a consequence of virtually nonexistent hysteresis loops. Data collected for this task showed tight, completely reversible load-elongation plots. This characteristic implies that global thermal equilibrium is

achieved at some time prior to the 39 hour mark on a whole mass basis. Local temperatures however may constantly vary as a function of load redistribution from fiber and tow failures.

Temperature data collected via the IR camera is shown for both the fatigue tests and the ultimate strength tests in Table 2.

Table 2 TEMPERATURES FROM FATIGUE TESTS

SLING #	TEMP. °F (observed)	TEMP. °F (ambient)	TEMP. °F DIFFERENCE	LOCATION/COMMENTS
5	92	80	12	splice
1	91	81	10	splice
2	88	78	10	potting
6	92	78	14	embedded thermocouple

TEMPERATURES FROM ULTIMATE STRENGTH TESTS

SLING #	TEMP. °F (observed)	TEMP. °F (ambient)	TEMP. °F DIFFERENCE	LOCATION/COMMENTS (temp. max)
3	111 120*	80 80	31 40	@ splice
5	116 123*	81 81	35 42	@ splice
1	97 126*	80 80	17 46	@ base of potting
2	120 128*	80 80	40 48	@splice and potting
6	117 121*	82 82	35 39	splice bunch pulled out
4	117 124*	81 81	36 43	splice bunch

NOTE: * indicates instant after failure

Heat dissipating at the surface of the sling legs was easily detected by the thermal imaging system. Surface temperatures obtained in Table 2 were calculated by using an emissivity value of 0.85. Temperatures monitored by embedded thermocouples were typically 3 to 5 degrees higher that those obtained by the camera and varied within this range throughout the tests.

Under flight simulation, the maximum observed temperatures were recorded during the 4.8G lift-off loads. A maximum temperature difference of 14 degrees Fahrenheit above ambient was measured within the splice region of sling #6.

During ultimate strength tests, male and female test specimens produced similar heat and temperature profiles. Average values determined by the thermal imager prior to failure were 33 degrees Fahrenheit +/- 7 above ambient compared to 43 degrees Fahrenheit +/- 3 at failure. Failure temperatures reported in Table 2 were extrapolated as a consequence of exceeding prefailure test system scales.

As shown by the data above, observed temperatures during the fatigue tests did not approach the critical failure temperatures as advertised by SPECTRA manufacturers (approx. 120 deg. C). High temperatures observed during the ultimate strength tests are most likely the result of released strain energy at the instant of failure. Prefailure (operating) and ultimate strength test temperatures both demonstrate a load-temperature relationship. It is likely that temperatures higher than those observed during testing were achieved at local friction interfaces possibly resulting in localized melting.

OBSERVATIONS

Visual observations of the potting, splice, and loop areas were made after each failed specimen was removed from the test machine. Radiographs of the potted loop areas of failed slings were taken for comparing pre and post failure geometry. Male test specimens consistently retained the original "loop shape" after load removal. In contrast, female test specimens consistently demonstrated a high degree of constriction or "bunching-up" throughout the loop section and retained this shape after failure. Post failure photographs contrasting male and female test specimens were taken and are shown in Figures 6a,b,c. In each of these photographs, the male specimen is shown on the left side and the female on the right.

For all the potted specimens, regardless of male/female test legs, portions of the splices were torn from the potting area with sections of the potting compound bonded to the cable surface. Close to these areas, a high degree of torn and frayed fibers were present. On some cables, broken fibers demonstrated the hard nodular ends that were observed earlier during the "forward sling accident specimen" analysis.

CONCLUSIONS

The most significant result or observation obtained from these tests was the similarity among the geometry of the three male specimens in contrast to the geometry of the three female specimens. Videotape recordings show that the accident initiated by failure of the forward sling. The recovered forward sling shares similar geometric characteristics to all three failed males. Calculations performed on data obtained from these tests show that male legs, with their higher spring stiffness, carry a significantly higher percent of the load. These results imply that loads in EAT applications may not be evenly distributed and that the forward sling failed by achieving the maximum load capacity of the male leg.

In EAT applications, slings are first mounted to the cargo lift points and then attached to the helicopter hooks. If rigging procedures are such that the male legs are diagonally opposed in the four point lift configuration, then the effects of fatigue may be amplified as the cargo oscillates about the two male legs due to the greater elongation capability in the female legs.

Test results also indicate that virgin specimens have a lower spring stiffness as compared to fatigued specimens (no reference to male/female gender). This evidence suggests that reaction forces from vibration induced loads are amplified in slings having higher hours of service.

Splices torn from the potting material showed a marginal degree of fiber abrasion after 40 hours of fatigue. It would appear that local friction causes some degradation of the fibers near the splice, but it is unclear whether this is sufficient to cause failure. Furthermore it would be difficult to identify whether melting occurred before failure or as a result of the failure through the release of strain energy or by friction as the cable slipped out of the potting compound. The black potting compound has a very rough internal surface and would act to abrade the cable. In addition, the black color would absorb heat and exacerbate any temperature effects. Compounding this problem is the fact that these SPECTRA cables are manufactured with a "weave" or "braid" pattern which assists in distributing axial loads throughout the cable cross section. Therefore, load redistribution at critical areas such as the splice (where sling legs are split) may be restricted because of potting interference. In field service, where slings are subjected to higher temperatures from direct sunlight and contaminants such as salt crystals, fiber abrasion rates are most likely accelerated thereby resulting in a further amplification of forces in the remaining load bearing tows.

ACKNOWLEDGEMENTS

The authors of this report would like to express their appreciation for the assistance and expertise offered by the following individuals.

Mr. C. E. Freese of ARL-MD for his comments regarding mechanics related issues of the splice. Mr. Dana Granville of ARL-MD for his support in materials applications related issues. Dr. Walter X. Zukas, Mr. David A. Bulpett and Dr. James M. Sloan, also from ARL-MD, for determining material properties by means Differential Scanning Calorimetry and Fourier Transform-Infra Red Spectroscopy.

Special thanks to Mr. Andrew Maun III and Mr. Sean Wellman of NRDEC for their participation in organizing the logistics and researching the facts of the failure. Also, thanks to Mr. Steven Chamberlin for his contributions in directing the organization of the various agencies involved and for providing background information and data as necessary.

TABLE OF FIGURES

	Page
Figure 1. Spectra Airlift Sling System.	14
Figure 2. Samson Brummell Slice	15
Figure 3. Specimen Removed by Water Jet	16
Figure 4. Schematic Diagram of Assymetric Test Set-Up . .	17
Figure 5a. Practice Test (I).	18
Figure 5b. Practice Test (II).	19
Figure 6. Photographs of Failed Slings.	20

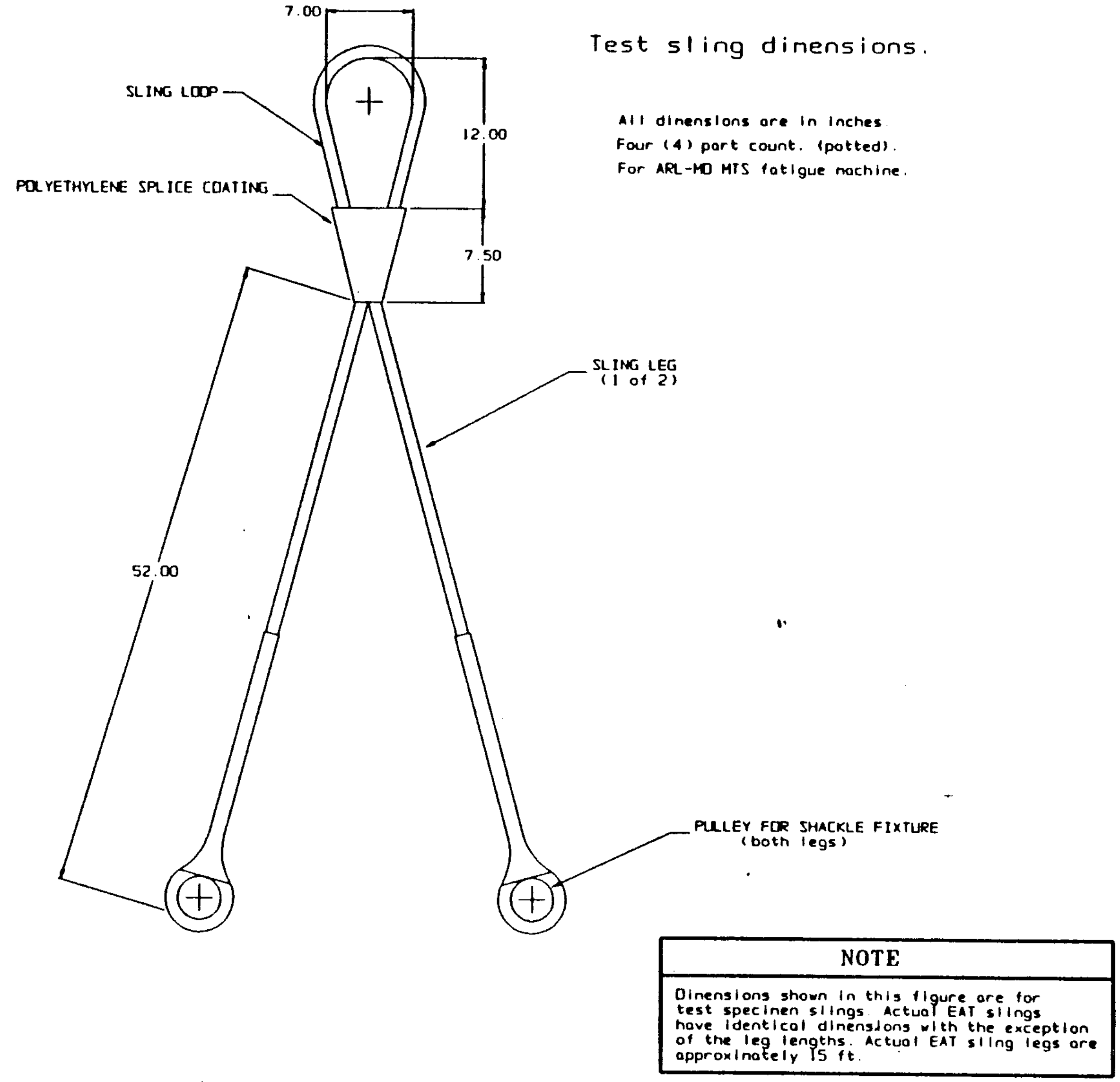

Figure 1. SPECTRA^{TM} Airlift Sling System.

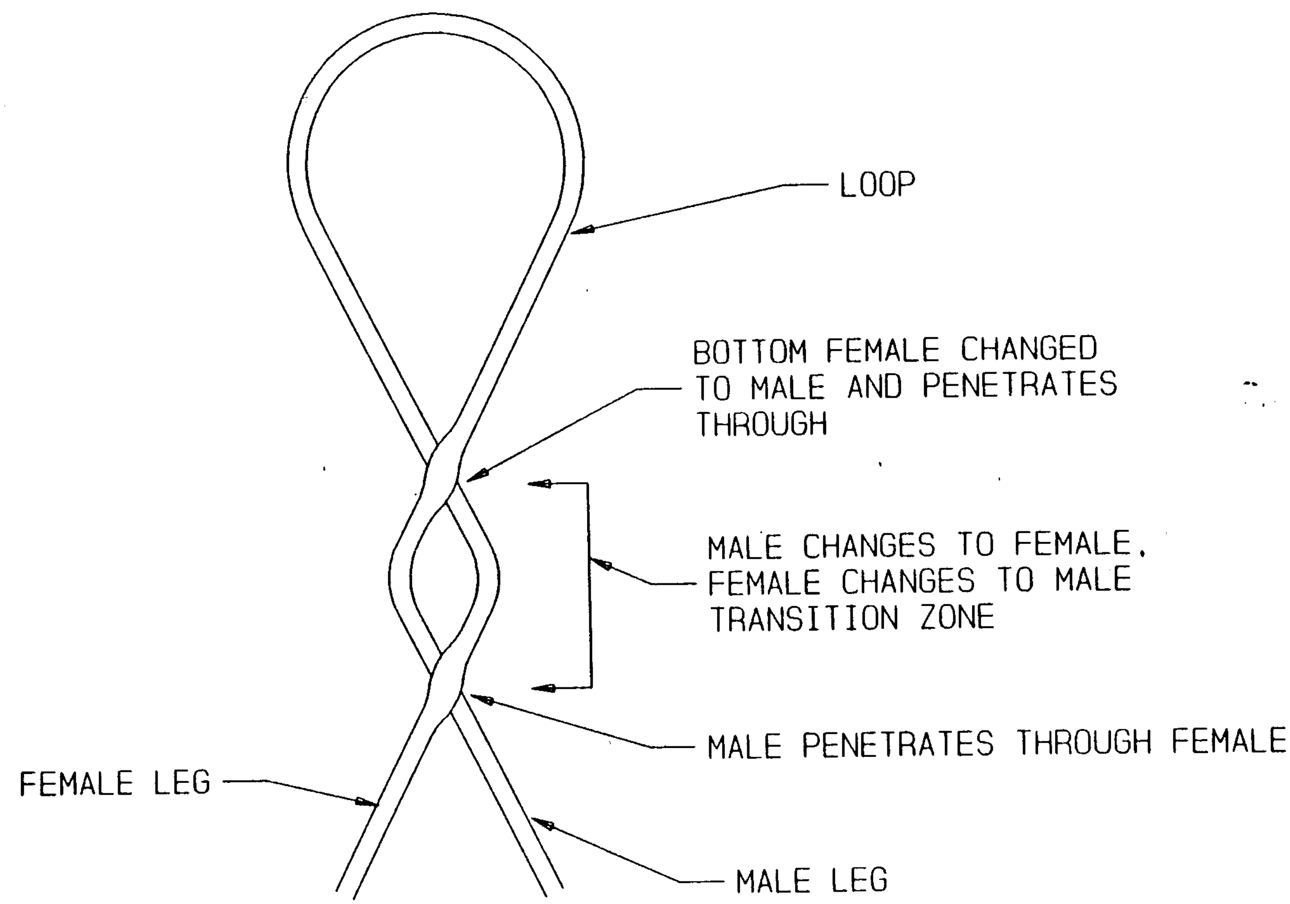

Figure 2. Samson Brummell Splice.

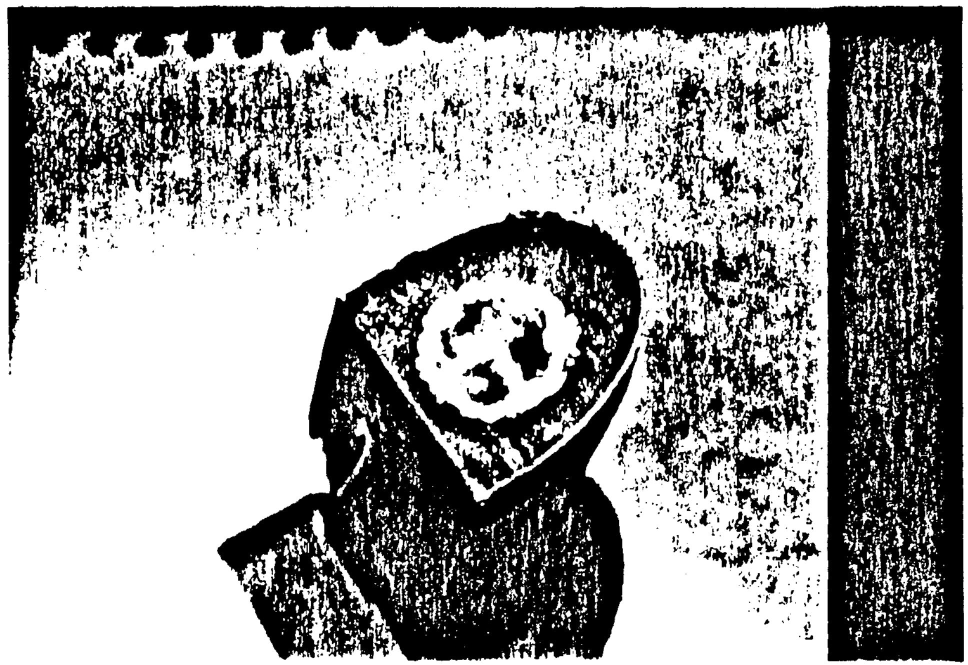

Figure 3. Specimen removed by water jet.

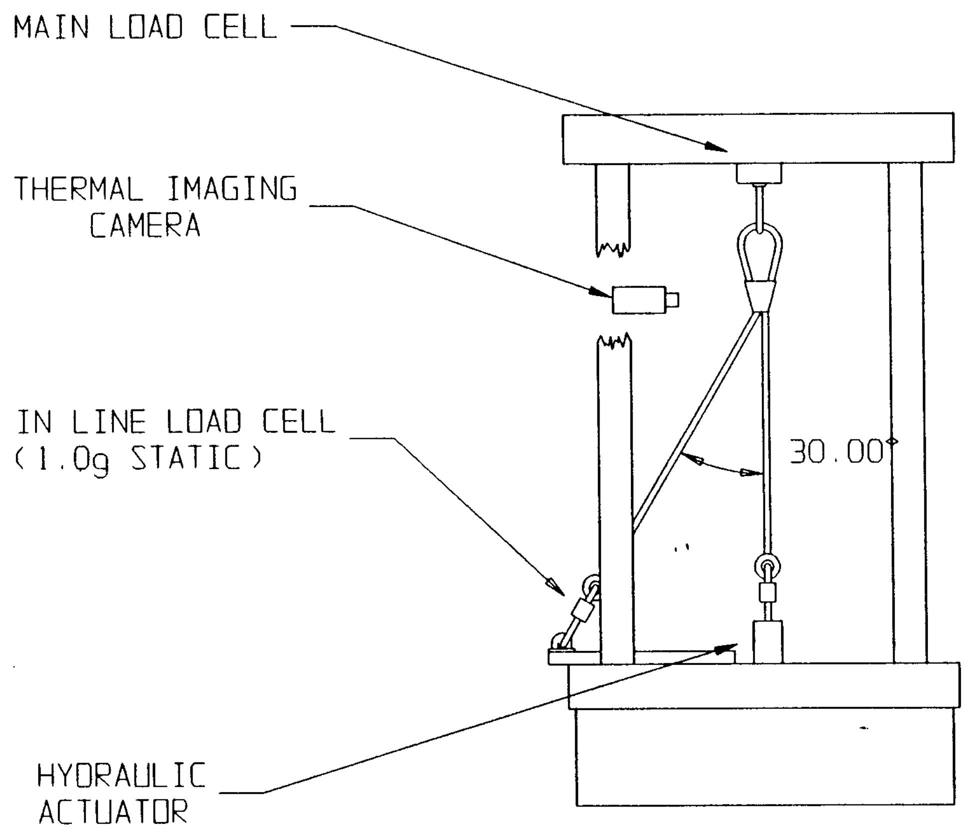

Figure 4. Schematic diagram of sling positioned in test machine for fatigue loading.

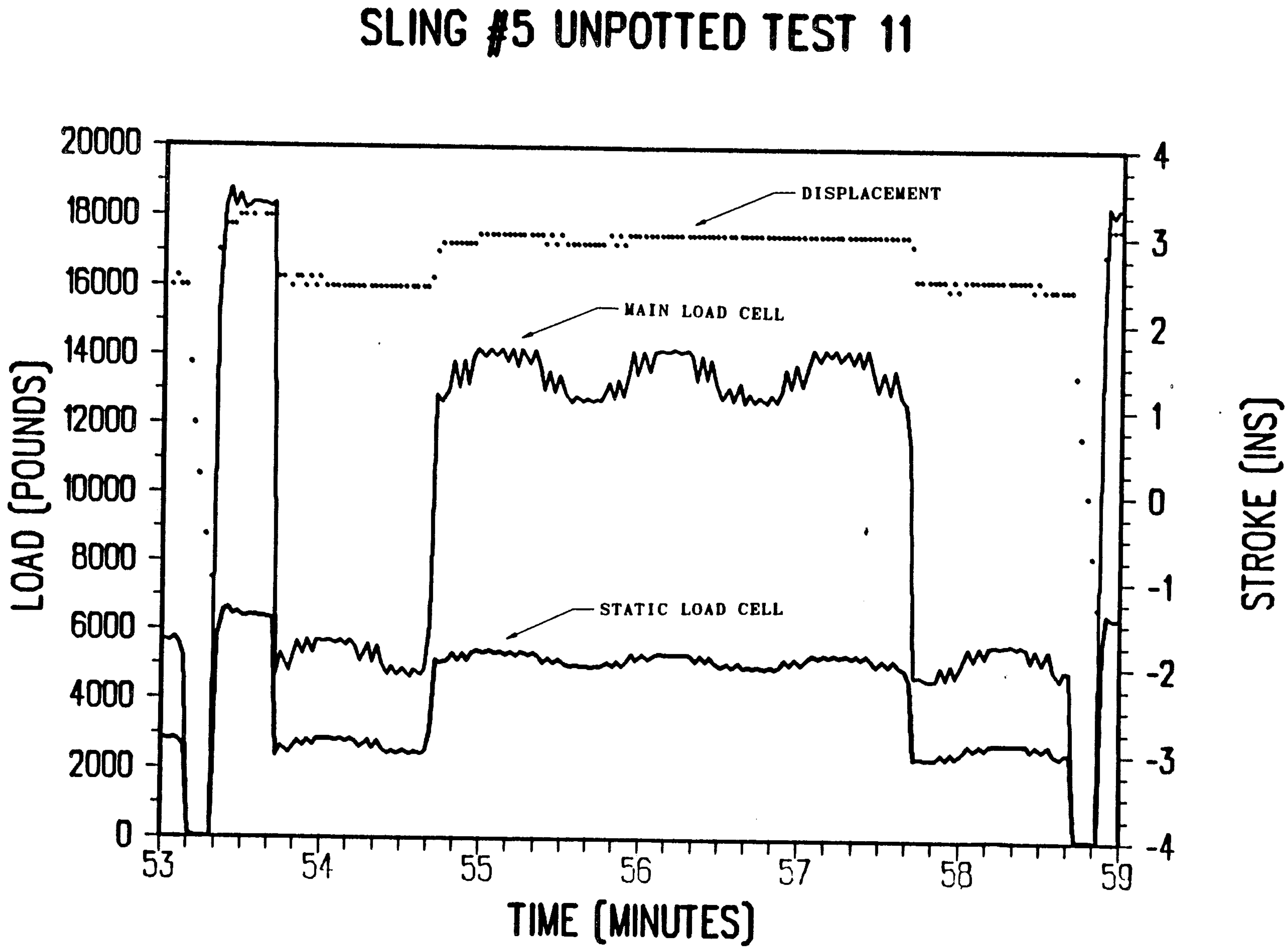

Figure 5a. Practice test: load cell output and stroke versus time.

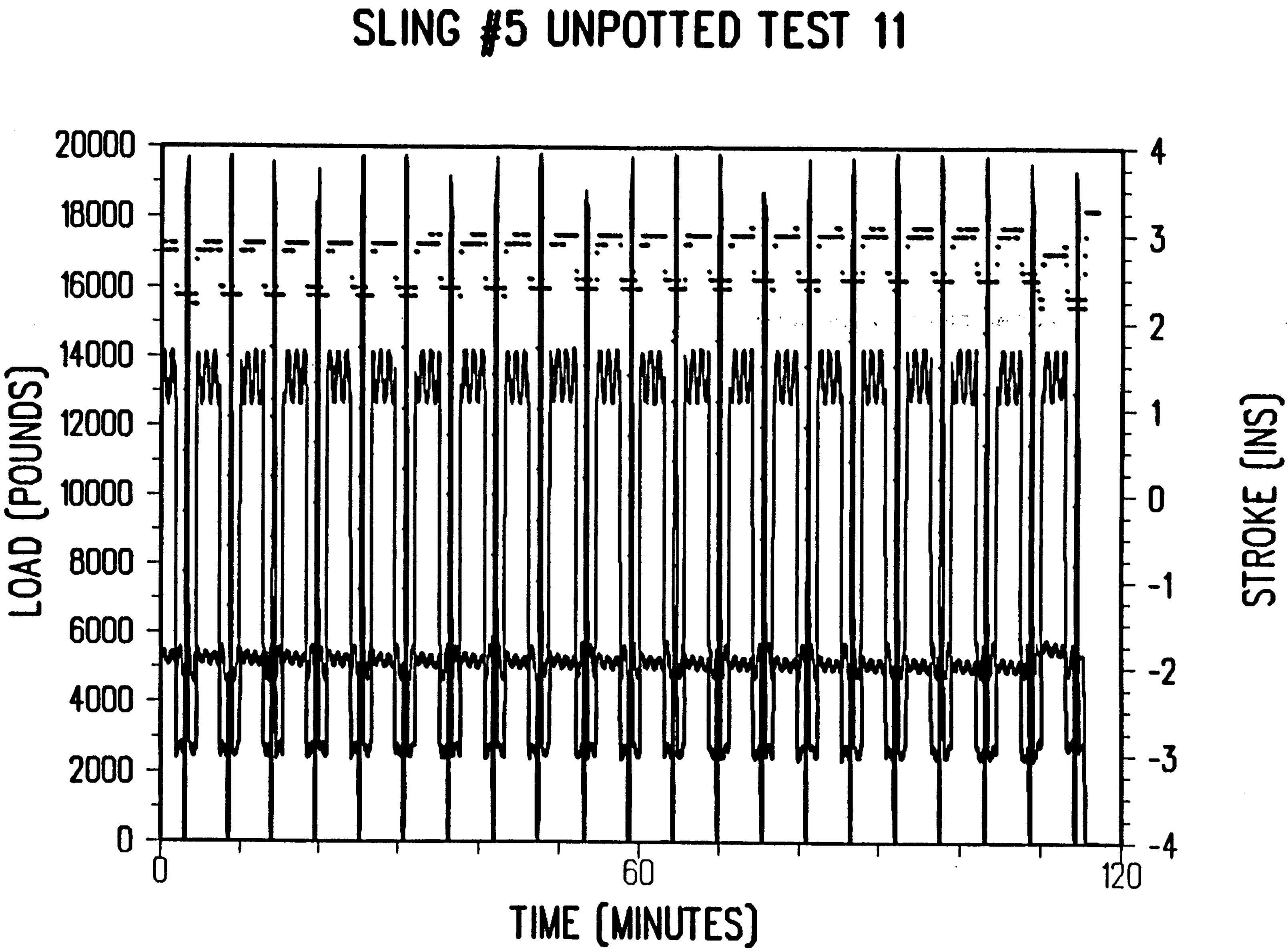

Figure 5b. Practice test: load cell output and stroke versus time.

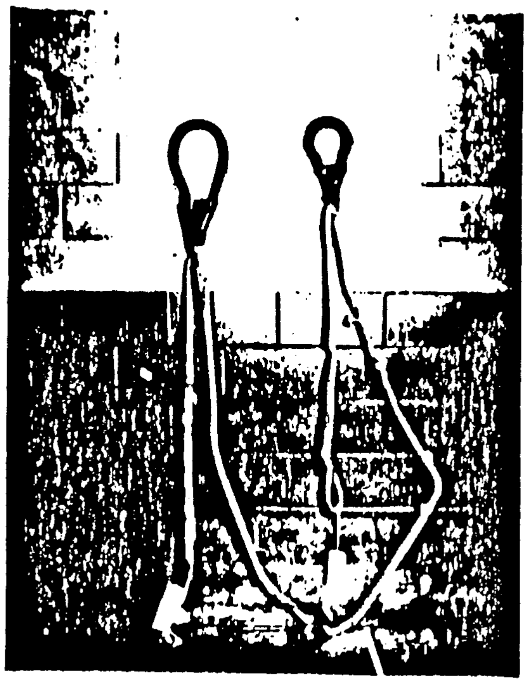

Fig. 6a.

left: sling #2 (male)
right: sling #1 (female)

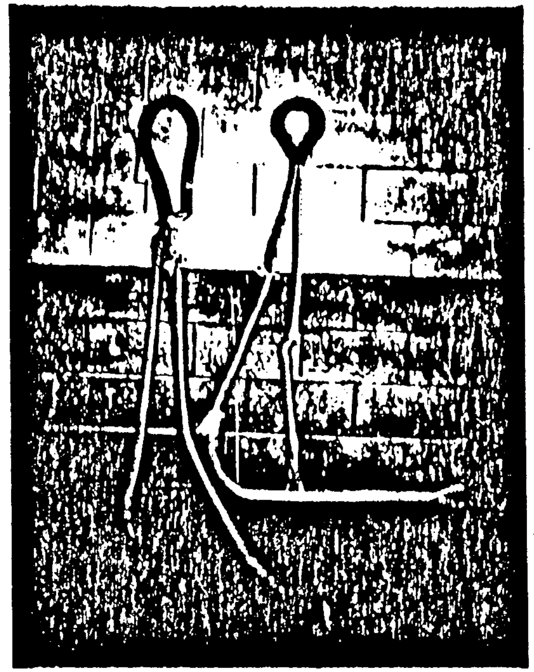

Fig. 6b.

left: sling #4 (male)
right: sling #3 (female)

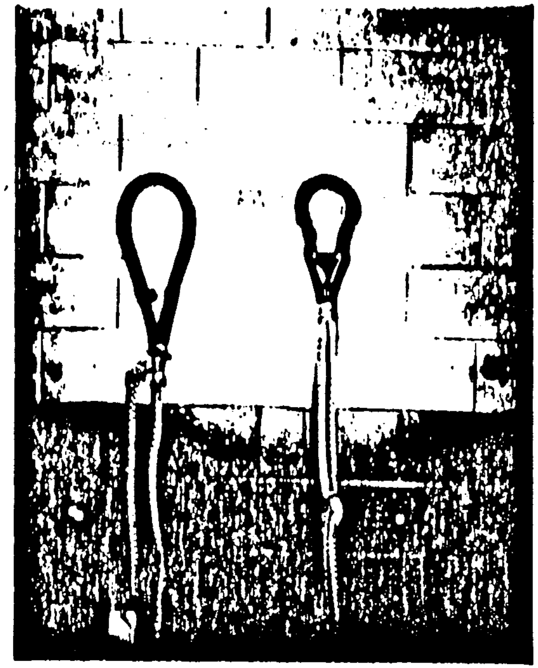

Fig. 6c.

left: sling #6 (male)
right: sling #5 (female)

Figure 6. Photographs of failed slings.

APPENDIX I

Thermodynamic Properties and Chemical Identification

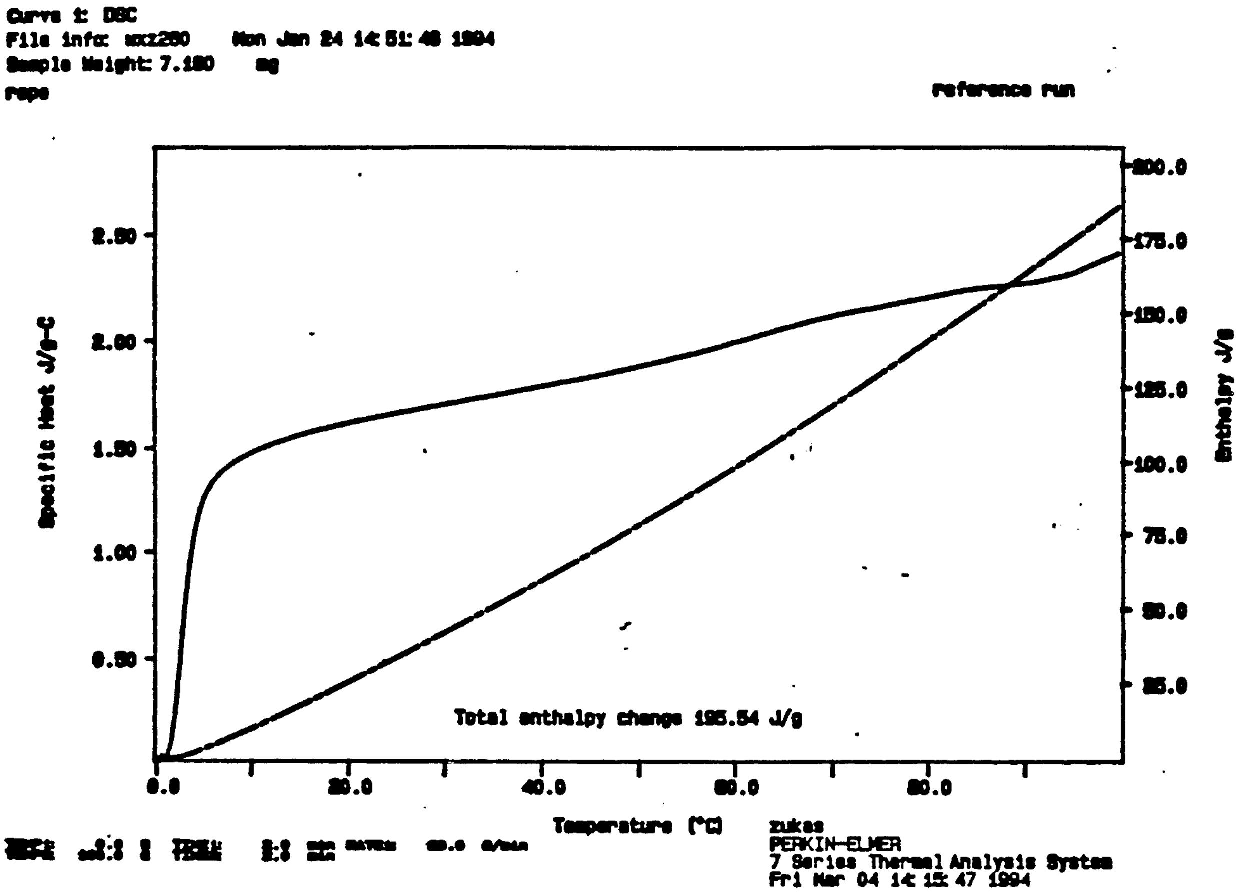

SPECIFIC HEAT

SAMPLE INFORMATION:
DSC Data File: wxz260
Sample Weight 7.180 mg
Mon Jan 24 14:51:48 1994
rope

REFERENCE INFORMATION:
DSC Data File: wxz259
Mon Jan 24 13:57:42 1994
reference run
Temp1 0.000 C
Temp2 100.000 C
Time1 2.000 min
Time2 2.000 min
Rate 20.000 C/min
Ro 62.000 C/W (user input)

TEMPERATURE (Deg C)	SPECIFIC HEAT (J/g-C)	ENTHALPY (J/g)
0.000	0.031	0.016
10.000	1.478	10.540
20.000	1.616	26.179
30.000	1.704	42.846
40.000	1.789	60.367
50.000	1.882	78.771
60.000	1.997	98.223
70.000	2.120	118.922
80.000	2.208	140.637
90.000	2.275	163.149

Results of Differential Scanning Calorimetry (DSC) tests of Spectra material.

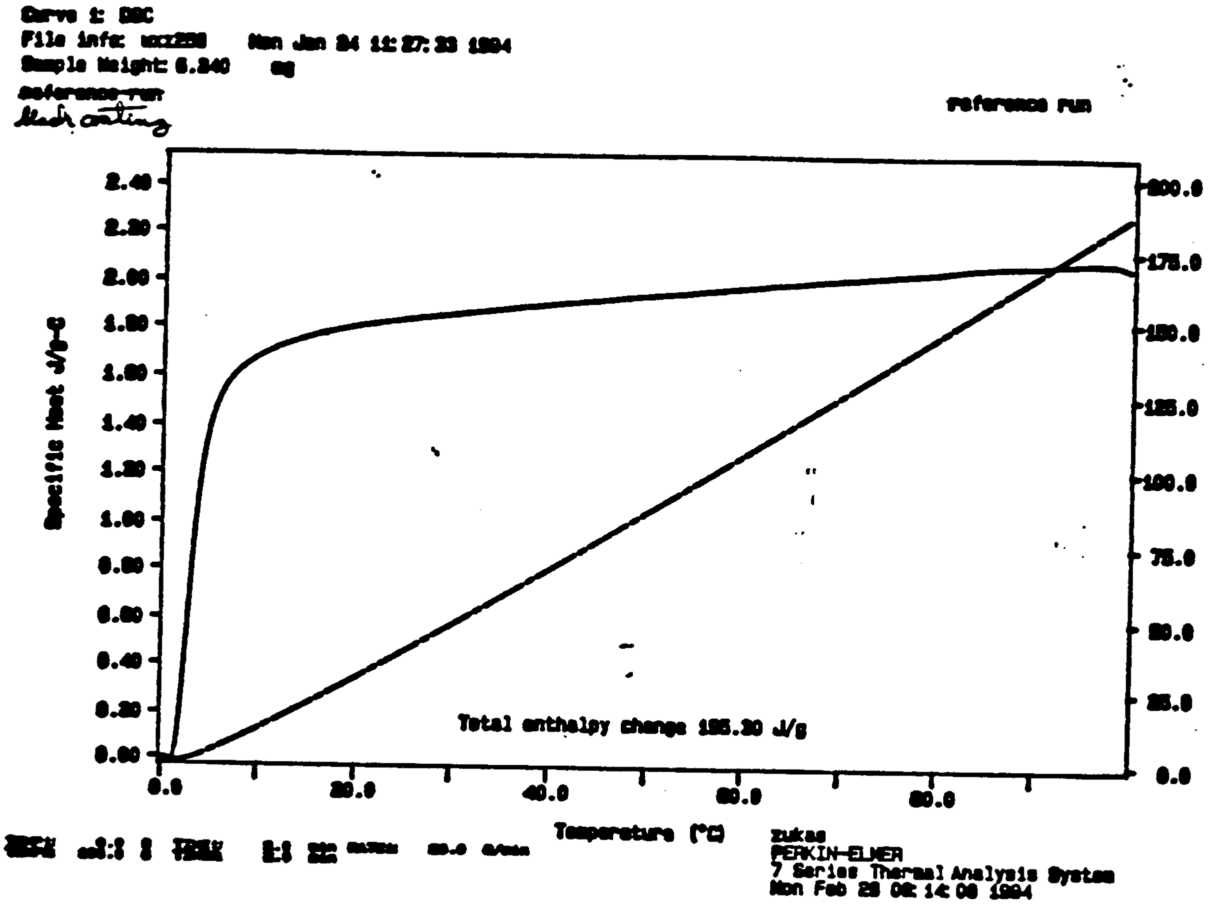

SPECIFIC HEAT

SAMPLE INFORMATION:
DSC Data File: wxz258
Sample Weight 6.240 mg
Mon Jan 24 11:27:33 1994
~~reference run~~
black coating

REFERENCE INFORMATION:
DSC Data File: wxz257
Mon Jan 24 11:04:21 1994
reference run

Temp1	0.000 C	
Temp2	100.000 C	
Time1	2.000 min	
Time2	2.000 min	
Rate	20.000 C/min	
Ro	62.000 C/W	(user input)

TEMPERATURE (Deg C)	SPECIFIC HEAT (J/g-C)	ENTHALPY (J/g)
0.000	6.043e-004	-3.457e-005
10.000	1.685	11.697
20.000	1.810	29.366
30.000	1.863	47.791
40.000	1.906	66.671
50.000	1.945	85.950
60.000	1.980	105.592
70.000	2.017	125.614
80.000	2.050	145.974
90.000	2.076	166.668

Results of Differential Scanning Calorimetry (DSC) tests of potting compound.

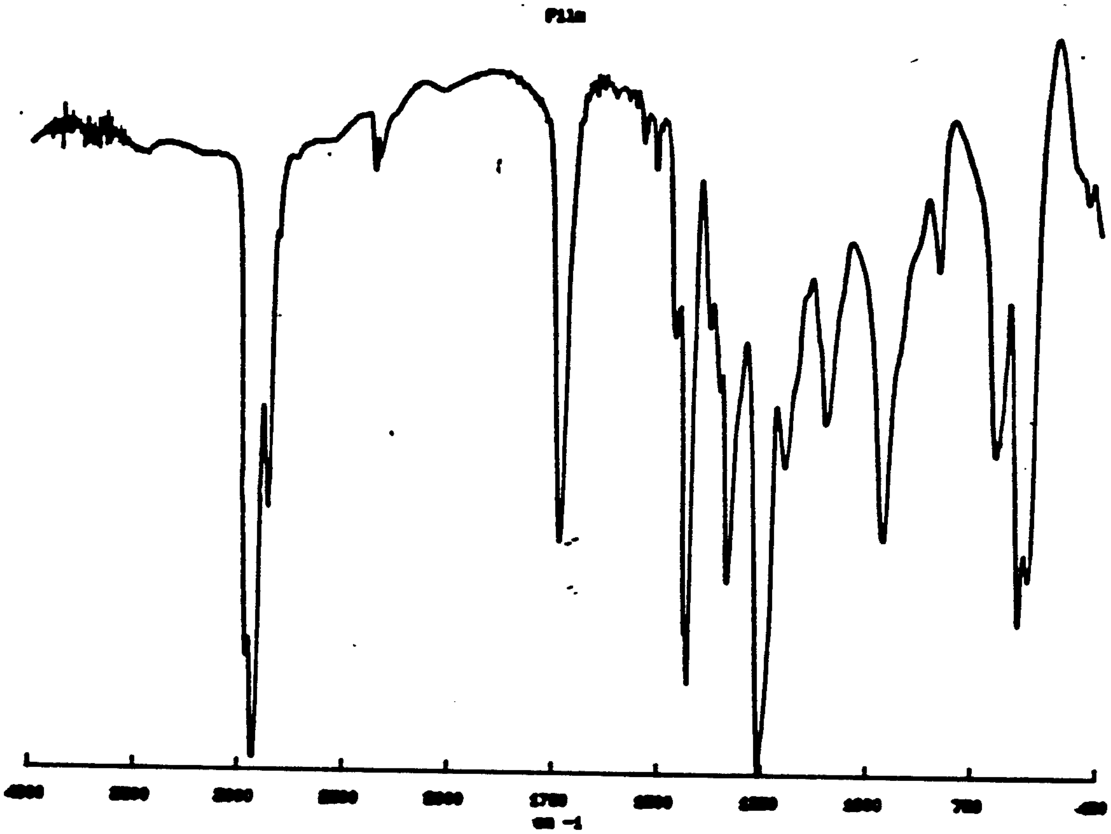

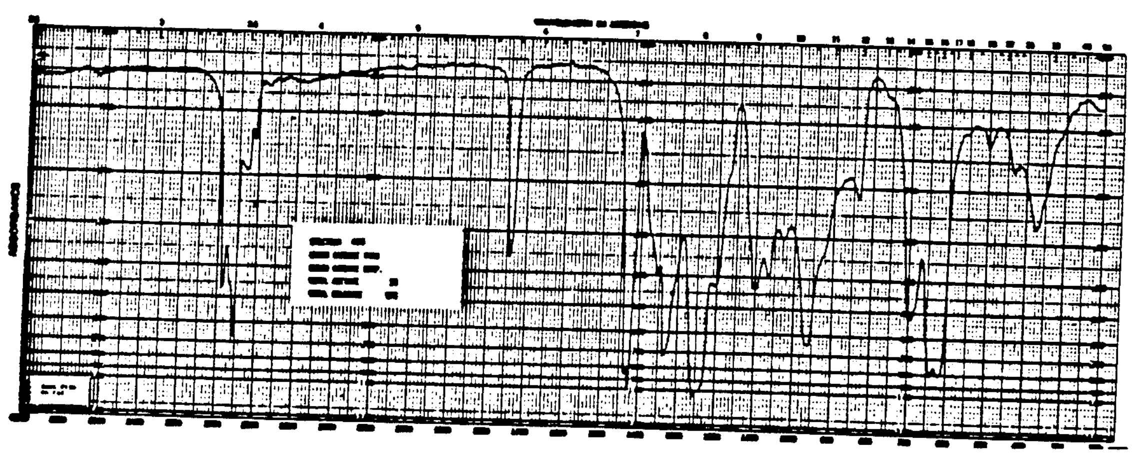

ABOVE: FT-IR spectroscopy results of film material removed from inside the failed forward loop.
BELOW: FT-IR spectroscopy calibration spectrum. Results indicate the material is vinyl chloride.

DISTRIBUTION LIST

No. of Copies	To
1	Office of the Under Secretary of Defense for Research and Engineering, The Pentagon, Washington, DC 20301
	Director, U.S. Army Research Laboratory, 2800 Powder Mill Road, Adelphi, MD 20783-1197
1	ATTN: AMSRL-OP-SD-TP, Technical Publishing Branch
1	AMSRL-OP-SD-TA, Records Management
1	AMSRL-OP-SD-TL, Technical Library
	Commander, Defense Technical Information Center, Cameron Station, Building 5, 5010 Duke Street, Alexandria, VA 23304-6145
2	ATTN: DTIC-FDAC
1	MIA/CINDAS, Purdue University, 2595 Yeager Road, West Lafayette, IN 47905
	Commander, Army Research Office, P.O. Box 12211, Research Triangle Park, NC 27709-2211
1	ATTN: Information Processing Office
	Commander, U.S. Army Materiel Command, 5001 Eisenhower Avenue, Alexandria, VA 22333
1	ATTN: AMCSCI
1	AMCMI-IS-A
	Commander, U.S. Army Materiel Systems Analysis Activity, Aberdeen Proving Ground, MD 21005
1	ATTN: AMXSY-MP, H. Cohen
	Commander, U.S. Army Missile Command, Redstone Arsenal, AL 35809
1	ATTN: AMSMI-RD-CS-R/Doc
	Commander, U.S. Army - ARDEC, Information Research Center, Picatinny Arsenal, NJ 07806-5000
1	ATTN: AMSTA-AR-IMC, Bldg. 59
	Commander, U.S. Army Natick Research, Development and Engineering Center Natick, MA 01760-5010
1	ATTN: SATNC-MI, Technical Library
1	SATNC-AI
	Commander, U.S. Army Satellite Communications Agency, Fort Monmouth, NJ 07703
1	ATTN: Technical Document Center
	Commander, U.S. Army Tank-Automotive Command, Warren, MI 48397-5000
1	ATTN: AMSTA-ZSK
1	AMSTA-TSL, Technical Library
1	AMSTA-SF
	President, Airborne, Electronics and Special Warfare Board, Fort Bragg, NC 28307
1	ATTN: Library

No. of Copies	To
	Director, U.S. Army Research Laboratory, Weapons Technology, Aberdeen Proving Ground, MD 21005-5066
1	ATTN: AMSRL-WT
2	Technical Library
	Commander, Dugway Proving Ground, UT 84022
1	ATTN: Technical Library, Technical Information Division
	Commander, U.S. Army Research Laboratory, 2800 Powder Mill Road, Adelphi, MD 20783
1	ATTN: AMSRL-SS
	Director, Benet Weapons Laboratory, LCWSL, USA AMCCOM, Watervliet, NY 12189
1	ATTN: AMSMC-LCB-TL
1	AMSMC-LCB-R
1	AMSMC-LCB-RM
1	AMSMC-LCB-RP
	Commander, U.S. Army Foreign Science and Technology Center, 220 7th Street, N.E., Charlottesville, VA 22901-5396
3	ATTN: AIFRTC, Applied Technologies Branch, Gerald Schlesinger
	Commander, U.S. Army Aeromedical Research Unit, P.O. Box 577, Fort Rucker, AL 36360
1	ATTN: Technical Library
	U.S. Army Aviation Training Library, Fort Rucker, AL 36360
1	ATTN: Building 5906-5907
	Commander, U.S. Army Agency for Aviation Safety, Fort Rucker, AL 3636
1	ATTN: Technical Library
	Commander, Clarke Engineer School Library, 3202 Nebraska Ave., N., Fort Leonard Wood, MO 65473-5000
1	ATTN: Library
	Commander, U.S. Army Engineer Waterways Experiment Station, P.O. Box 631, Vicksburg, MS 39180
1	ATTN: Research Center Library
	Commandant, U.S. Army Quartermaster School, Fort Lee, VA 23801
1	ATTN: Quartermaster School Library
	Naval Research Laboratory, Washington, DC 20375
1	ATTN: Code 6384
	Chief of Naval Research, Arlington, VA 22217
1	ATTN: Code 471
	Commander, U.S. Air Force Wright Research and Development Center, Wright-Patterson Air Force Base, OH 45433-6523
1	ATTN: WRDC/MLLP, M. Forney, Jr.
1	WRDC/MLBC, Mr. Stanley Schulman

No. of Copies	To
	U.S. Department of Commerce, National Institute of Standards and Technology, Gaithersburg, MD 20899
1	ATTN: Stephen M. Hsu, Chief, Ceramics Division, Institute for Materials Science and Engineering
1	Committee on Marine Structures, Marine Board, National Research Council, 2101 Constitution Avenue, N.W., Washington, DC 20418
1	Materials Sciences Corporation, Suite 250, 500 Office Center Drive, Fort Washington, PA 19034
1	Charles Stark Draper Laboratory, 555 Technology Square, Cambridge, MA 02139
	General Dynamics, Convair Aerospace Division, P.O. Box 748, Fort Worth, TX 76101
1	ATTN: Mfg. Engineering Technical Library
	Plastics Technical Evaluation Center, PLASTEC, ARDEC, Bldg. 355N, Picatinny Arsenal, NJ 07806-5000
1	ATTN: Harry Pebly
1	Department of the Army, Aerostructures Directorate, MS-266, U.S. Army Aviation R&T Activity - AVSCOM, Langley Research Center, Hampton, VA 23665-5225
1	NASA - Langley Research Center, Hampton, VA 23665-5255
	U.S. Army Vehicle Propulsion Directorate, NASA Lewis Research Center, 2100 Brookpark Road, Cleveland, OH 44135-3191
1	ATTN: AMSRL-VP
	Director, Defense Intelligence Agency, Washington, DC 20340-6053
1	ATTN: PAQ-4B (Dr. Kenneth Crelling)
	U.S. Army Communications and Electronics Command, Fort Monmouth, NJ 07703
1	ATTN: Technical Library
	U.S. Army Research Laboratory, Electronic Power Sources Directorate, Fort Monmouth, NJ 07703
1	ATTN: Technical Library
	Director, U.S. Army Research Laboratory, Watertown, MA 02172-0001
2	ATTN: AMSRL-OP-WT-IS, Technical Library
5	Author